ACS Medicinal Chemistry Letters

Letter

pubs.acs.org/acsmedchemlett

Discovery of a Highly Selective, Brain-Penetrant Aminopyrazole LRRK2 Inhibitor

Bryan K. Chan,*[,†] Anthony A. Estrada,[†] Huifen Chen,[†] John Atherall,[⊥] Charles Baker-Glenn,[⊥] Alan Beresford,[▽] Daniel J. Burdick,[†] Mark Chambers,[⊥] Sara L. Dominguez,[∥] Jason Drummond,[‡] Andrew Gill,[#] Tracy Kleinheinz,[‡] Claire E. Le Pichon,[∥] Andrew D. Medhurst,[#] Xingrong Liu,[§] John G. Moffat,[‡] Kevin Nash,[#] Kimberly Scearce-Levie,[∥] Zejuan Sheng,[∥] Daniel G. Shore,[†] Hervé Van de Poël,[⊥] Shuo Zhang,[∥] Haitao Zhu,[∥] and Zachary K. Sweeney[†]

Departments of [†]Discovery Chemistry, [‡]Biochemical and Cellular Pharmacology, [§]Drug Metabolism and Pharmacokinetics, and [∥]Neuroscience, Genentech, Inc., 1 DNA Way, South San Francisco, California 94080, United States

Departments of [⊥]Chemistry, [#]Biochemical and Cellular Pharmacology, and [▽]Drug Metabolism and Pharmacokinetics, BioFocus, Chesterford Research Park, Saffron Walden, Essex CB10 1XL, United Kingdom

Supporting Information

ABSTRACT: The modulation of LRRK2 kinase activity by a selective small molecule inhibitor has been proposed as a potentially viable treatment for Parkinson's disease. By using aminopyrazoles as aniline bioisosteres, we discovered a novel series of LRRK2 inhibitors. Herein, we describe our optimization effort that resulted in the identification of a highly potent, brain-penetrant aminopyrazole LRRK2 inhibitor (**18**) that addressed the liabilities (e.g., poor solubility and metabolic soft spots) of our previously disclosed anilino-aminopyrimidine inhibitors. In in vivo rodent PKPD studies, **18** demonstrated good brain exposure and engendered significant reduction in brain pLRRK2 levels post-ip administration. The strategies of bioisosteric substitution of aminopyrazoles for anilines and attenuation of CYP1A2 inhibition described herein have potential applications to other drug discovery programs.

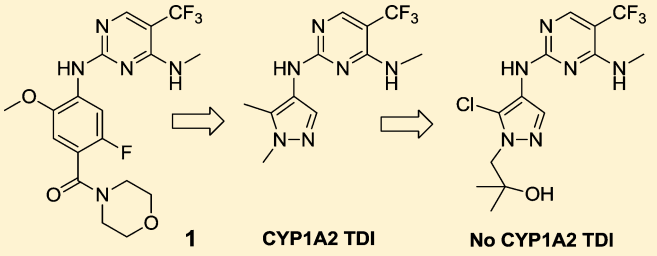

KEYWORDS: *LRRK2, kinase inhibitor, Parkinson's disease, CYP1A2 inhibition*

Parkinson's disease (PD) is a neurodegenerative disorder that affects approximately 1% of the world's population over the age of 65.[1] Identification of a disease-modifying or neuroprotective therapeutic for PD patients remains a significant challenge. Recently, genetic research has revealed a connection between a missense mutation (G2019S) in the leucine-rich repeat kinase 2 (LRRK2) gene and a number of familial and idiopathic PD cases.[2−9] Significantly, multiple reports have shown that this mutation enhances the kinase activity of LRRK2.[10−17] The modulation of LRRK2 kinase activity by a selective small molecule inhibitor has therefore been proposed as a potential treatment for PD.[18−23]

We recently reported the first disclosure of a series of highly potent, selective, and brain-penetrable anilino-pyrimidine LRRK2 inhibitors as exemplified by compound **1**.[22,23] Examination of the liabilities of **1** and structurally similar analogues revealed (a) moderate to poor aqueous solubility (thermodynamic solubility of **1** at pH 7.4 < 0.9 μg/mL), (b) potential for *ortho*-quinoneimine reactive metabolite formation, and (c) a morpholinocarboxamide motif as a major site of metabolism as indicated by metabolite identification studies (MetID). In an effort to improve upon **1** and mitigate potential safety risks, we initiated a campaign to identify a suitable bioisosteric replacement for the aniline functionality. This approach resulted in the discovery of a novel series of highly selective aminopyrazole LRRK2 inhibitors.

Docking experiments using a JAK-2-derived homology model of LRRK2 suggested that compound **1** binds in the ATP binding site of LRRK2 as shown in Figure 1.[22,23] In designing anilino-carboxamide replacements, we chose to retain the hinge binding diaminopyrimidine core as well as the C-5 trifluoromethyl group that interacts favorably with the methionine gatekeeper through van der Waal contacts. Additionally, our lead optimization efforts toward **1** established the importance of occupying the vector adjacent to the hinge-binding anilino N-H motif (methoxy group in **1**) for overall kinase selectivity.[22,23] The incorporation of this "selectivity handle" was one of the major considerations in the design of possible aniline replacements. Lastly, the morpholine carboxamide moiety occupies a solvent-exposed region of the active site. This provided a flexible substitution vector to modulate physicochemical and ADME properties. Because of their favorable physicochemical properties and synthetic tractability,

Received: September 24, 2012
Accepted: November 23, 2012

dx.doi.org/10.1021/ml3003007 | *ACS Med. Chem. Lett.* XXXX, XXX, XXX−XXX

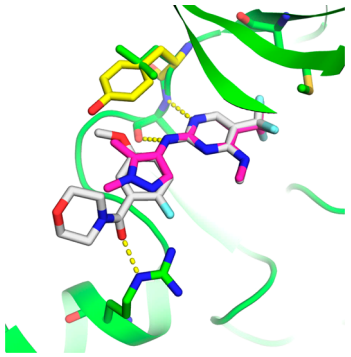

Figure 1. Docking model of **1** (gray) and **6** (pink) in LRRK2 binding site. Key hydrogen bonds are shown as yellow dashed lines. The side chain of Y931 of JAK2 is shown and colored in yellow.

aminopyrazoles were explored as potential bioisosteres for the aniline motif.[24,25]

The results of an initial screen of aminopyrazoles as aniline replacements are shown in Table 1. The inhibitors were also

Table 1. SAR of Pyrazole Isomers

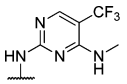

Cpd	R	LRRK2 Ki[a,c] (nM)	pLRRK2 IC_{50}[b,c] (nM)	JAK2 Ki / LRRK2 Ki
1	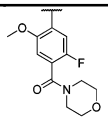	6	16	>530x
2		21	170	87x
3		11	130	>240x
4		41	99	2.7x
5		8	52	190x
6		2	41	560x
7		4	39	400x

[a]Biochemical assay. [b]Cellular assay.[27] [c]All IC_{50} values and apparent K_i values represent arithmetic means of at least two determinations. These assays generally produced results within 2-fold of the reported mean.

assayed for inhibition of Janus kinase 2 (JAK2), as previous efforts had confirmed that JAK2/LRRK2 biochemical selectivity correlated with biochemical selectivity against the broader kinome.[22,23] The 3- and 5-amino-linked pyrazoles (**2** and **3**) demonstrated good JAK2/LRRK2 selectivity but appeared to have inferior potency for LRRK2 in our biochemical screen and cell-based LRRK2 autophosphorylation assay when compared to the 4-linked aminopyrazoles (**5**−**7**). The poor JAK2 selectivity of compound **4** (2.7×) confirmed that a nitrogen lone pair (e.g., compound **2**) or 3-/5-substituent was required to achieve good selectivity. An overlap of docked structures **6** (pink) with **1** (gray) in our LRRK2 homology model is shown in Figure 1. As expected, the aminopyrazole coincided with the aniline of **1**, with the C5-methyl group (pyrazole numbering) directed toward the selectivity pocket and the *N*1-methyl toward solvent.

Compounds **5**−**7**, along with their ethyl and isopropyl analogues (**8**−**11**, Table 2), were profiled further in in vitro ADME assays. In general, the *N*-alkyl pyrazoles demonstrated moderate stability in human and rat liver microsomes (LM). Permeability assays using a MDR1-transfected MDCK cell line suggested that the pyrazole inhibitors were generally not human P-glycoprotein (Pgp) substrates (efflux ratio < 3). Disappointingly, however, compounds **5** and **7**−**11** were found to be reversible and/or time-dependent inhibitors of cytochrome P450 (CYP) 1A2.[26] This phenomenon proved to be a general trend for our first-generation aminopyrazole inhibitors.

A typical strategy to attenuate inhibition of the CYP family of enzymes includes modulating the affinity of the molecules toward the CYP enzymes by reducing lipophilicity.[28] Introduction of polar functionalities, such as methoxy and nitrile groups (compounds **12**−**15**), however, did not resolve the issue of CYP1A2 inhibition.

Established SAR of known substrates and inhibitors of CYP1A2 suggests that the CYP1A2 binding site is extremely compact.[29,30] We therefore opted to take advantage of the uniquely shaped active site of CYP1A2 in our optimization effort. It was hypothesized that reduced CYP1A2 inhibition could be achieved through the introduction of sterically demanding groups that would engender steric clashes with the planar and narrow CYP1A2 active site.

With the high degree of structural tolerability, bulky three-dimensional substitutions at the solvent-exposed pyrazole N-capping group were explored further. Toward this end, a *gem*-dimethyl group was introduced onto the cyanoethyl motif of compound **15**, one of the least lipophilic analogues [cLogP = 1.9; lipophilic ligand efficiency (LLE) = 6.3] from our initial screen. We were pleased to find that dimethylated analogue **16** maintained its affinity for LRRK2, and the metabolic stability was not compromised despite the increase in lipophilicity (cLogP = 2.6; LLE = 5.9). More importantly, **16** demonstrated no reversible or time-dependent inhibition (TDI) of CYP1A2. Replacement of the nitrile with a hydroxyl group (**17**) further improved metabolic stability without evidence of CYP1A2 inhibition.

When dosed intravenously at 0.5 mg/kg in rat, **17** demonstrated moderate clearance and a modest unbound brain to unbound plasma area under the curve (AUC) ratio (Table 3). In vitro LM MetID studies of related compounds have shown oxidation of the C5-methyl of the pyrazole motif as one of the major routes of metabolism. To maintain favorable physicochemical properties, it was envisioned that the conversion of the methylpyrazole to chloropyrazole should obviate the metabolic liability.

Gratifyingly, chloropyrazole **18** showed improved in vivo brain exposure and stability in comparison to methylpyrazole **17**. Further in vivo PK studies in dogs with **18** demonstrated acceptable clearance and oral bioavailability. It is worthy of note that, despite the potential for the displacement of the chloro

dx.doi.org/10.1021/ml3003007 | ACS Med. Chem. Lett. XXXX, XXX, XXX−XXX

Table 2. SAR of Aminopyrazole Analogues

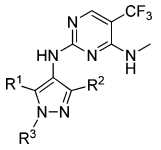

Cpd	R^1	R^2	R^3	LRRK2 Ki[a] (nM)	LM Cl_{hep}[b] H/R (mL/min/kg)	MDR1-MDCK A:B	ER[c] (B:A/A:B)	CYP1A2 IC_{50} (μM)	Evidence of CYP1A2 TDI[d]
5	H	Me	Me	8	9/9	5	1.4	0.7	YES
6	Me	H	Me	2	12/14	13	1.0	>10	NO
7	Cl	H	Me	4	16/24	2	2.3	5.8	NO
8	H	Me	Et	6	8/32	8	1.8	0.4	NO
9	Me	H	Et	2	11/26	15	1.6	4.7	YES
10	H	Me	*i*Pr	6	9/47	12	0.9	0.7	YES
11	Me	H	*i*Pr	3	7/41	13	0.9	3.1	NO
12	H	Me	CH_2CH_2OMe	6	9/21	12	0.8	1	NO
13	Me	H	CH_2CH_2OMe	2	4/24	17	1.4	>10	YES
14	H	Me	CH_2CH_2CN	5	11/18	7	3.5	5.2	YES
15	Me	H	CH_2CH_2CN	6	9/33	16	2.8	>10	YES
16	Me	H	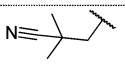	3	6/28	6	0.9	>10	NO
17	Me	H	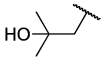	9	4/12	4	2.6	>10	NO
18	Cl	H		9	3/13	15	0.9	>10	NO

[a]Biochemical assay. All apparent K_i values represent arithmetic means of at least two determinations. These assays generally produced results within 2-fold of the reported mean. [b]LM predicted hepatic clearance. [c]ER measured in MDCK-MDR1 permeability assay. [d]Evidence of time-dependent inhibition includes either an IC_{50} of less than 10 μM or an increase in AUC of >30% in a IC_{50}-shift assay.

Table 3. In Vivo Pharmacokinetic Parameters

	rats PK[a]			dogs PK[b]	
compd	Cl_p (mL/min/kg)	V_d (L/kg)	B_u/P_u[c]	Cl_p (mL/min/kg)	*F* (%)
17	35	0.88	0.26		
18	21	2.5	0.37	22	31

[a]Compounds were dosed in male Sprague−Dawley rat at 0.5 mg/kg iv as a 60% NMP solution (n = 3). [b]Compound **18** was dosed in male Beagle dog at 0.5 mg/kg iv as a 30% NMP solution and at 1 mg/kg po as a 1% RC591 + 0.2% tween80 aqueous suspension (n = 3). [c]Unbound brain/unbound plasma AUC ratio determined after 0.5 mg/kg iv dose.

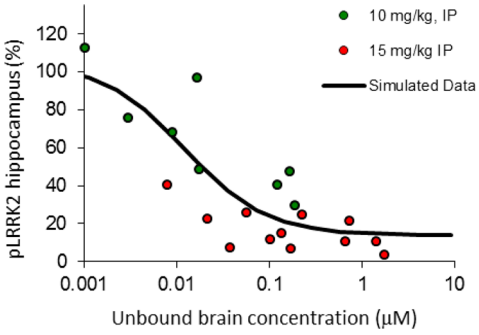

Figure 2. In vivo G2019S LRRK2 transgenic mouse PK/PD results measuring brain pSer1292 autophosphorylation. The circles represent the observed data for mice treated with **18**, and the line represents the predicted data from a direct inhibition model. The percent inhibition is normalized to pSer1292 levels observed in mice dosed with vehicle alone (n = 3).[32]

substituent by nucleophiles, incubation of **18** in human LMs in the presence of glutathione, KCN, or methoxyamine did not result in any observable conjugates.

Compound **18** exhibited good cellular potency (cell IC_{50} = 28 nM). When screened at 1 μM (116-fold over LRRK2 K_i) against a 185-membered Invitrogen kinase panel, compound **18** demonstrated inhibitory activity of >75% against only one other kinase (TSSK1, 75.2%). Additionally, the thermodynamic solubility at pH 7.4 was measured to be 20 μg/mL.

The pharmacodynamic effect of compound **18** was tested in bacterial artificial chromosome (BAC) transgenic mice expressing G2019S mutant LRRK2 gene.[31,32] As shown in Figure 2, robust concentration-dependent knockdown of phospho-LRRK2 (pLRRK2) levels in the brain was observed after ip dosing at 10 or 15 mg/kg. Inhibition modeling indicates the in vivo unbound brain IC_{50} of **18** to be 12 nM.[32]

The pyrazole-based LRRK2 analogues were synthesized according to Schemes 1 and 2. In Scheme 1, alkylation of 5-methyl-3-nitropyrazole (**19**) followed by hydrogenation afforded the corresponding aminopyrazoles (**20**). Acid- or palladium-catalyzed coupling of the aminopyrazole to 2-chloro-4-methylamino-5-trifluoromethylpyrimidine (**21**) provided the target compounds. Key pyrazole building blocks **25** and **27** were prepared as described in Scheme 2 using standard chemistry.

The incorporation of 2-alkoxyaniline motifs into the design of small molecule kinase inhibitors has become a common

dx.doi.org/10.1021/ml3003007 | ACS Med. Chem. Lett. XXXX, XXX, XXX−XXX

Scheme 1[a]

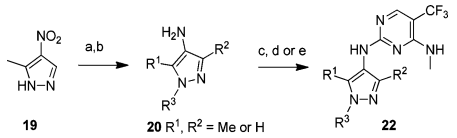

[a](a) R^3-Br, Cs_2CO_3, DMF, rt−100 °C, 0−3 h. (b) H_2, Pd/C, EtOH, 1−24 h. (c) Compound **21**, *n*-BuOH, μW, 140 °C, 20−60 min. (d) Compound **21**, TFA, $MeOCH_2CH_2OH$, 90 °C, 0.5−2 h. (e) Compound **21**, $Pd_2(dba)_3$, XPhos, Cs_2CO_3, DMF, 100 °C, 18 h.

Scheme 2[a]

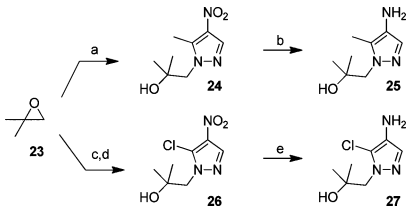

[a](a) Compound **19**, Cs_2CO_3, DMF, 100 °C, 3 h. (b) H_2, Pd/C, EtOH, rt, 20 h. (c) 4-Nitropyrazole, Cs_2CO_3, DMF, 100 °C, 3.5 h. (d) (i) LHMDS, THF, −70 °C, 25 min; (ii) C_2Cl_6, THF, −78 °C, 2.5 h. (e) Fe, NH_4Cl, EtOH, H_2O, 80 °C, 18 h.

strategy to achieve broad kinome selectivity.[33−36] In this paper, we described the use of aminopyrazoles as effective bioisosteres for the aniline motif. Through this strategy, we discovered the novel, selective, and brain-penetrant LRRK2 inhibitor **18**. In addition to eliminating the aniline toxicophore, inhibitor **18** exhibited a marked improvement in solubility as compared to **1** while maintaining excellent pharmacological and drug metabolism and pharmacokinetic profiles. Inhibitor **18** will be an effective tool to delineate the role of LRRK2 kinase activity in the etiology of PD. Moreover, during the optimization process, CYP1A2 inhibition was attenuated by incorporation of sterically demanding groups that engendered unfavorable interactions with the compact binding site of the enzyme. The general strategies of bioisosteric replacement of anilines with aminopyrazoles and attenuation of CYP1A2 inhibition described herein have potential applications to other drug discovery programs.

■ ASSOCIATED CONTENT

Supporting Information

Synthetic procedures, spectral data, and kinase selectivity data for key compounds and biological and ADME assay protocols. This material is available free of charge via the Internet at http://pubs.acs.org.

■ AUTHOR INFORMATION

Corresponding Author

*E-mail: chan.bryan@gene.com.

Present Address

Z.K.S.: Novartis Institutes for Biomedical Research, 4560 Horton Street, Emeryville, California 94608, United States.

Notes

The authors declare no competing financial interest.

■ ACKNOWLEDGMENTS

We thank the analytical, bioanalytical, NMR, pharmacokinetic, and biopharmacology colleagues for their assistance with compound purification and testing. We thank Dr. Zhenyu Yue and his group at the Mount Sinai School of Medicine for kindly providing the G2019S BAC transgenic mice. We also thank Linda Bao, Leo Berezhkovskiy, Po-Chang Chiang, Jonathan Cheong, Kang-Jye Chou, Xiao Ding, Claire Holt, Heather Kennedy, Emile Plise, Kimberley Smith, Hilda Solanoy, and Xiaolin Zhang for their individual contributions and Timothy Heffron for critical reading of this manuscript.

■ ABBREVIATIONS

AUC, area under the curve; *B*, brain concentration; BAC, bacterial artificial chromosome; B_u, unbound brain concentration; CYP, cytochrome P450; dba, dibenzylideneacetone; DMPK, drug metabolism and pharmacokinetics; ER, efflux ratio; GSH, glutathione; H, human; ip, intraperotineal; iv, intravenous; JAK2, Janus kinase 2; LHMDS, lithium hexamethyldisilazide; LLE, lipophilic ligand efficiency; LM, liver microsome; LRRK2, leucine-rich repeat kinase 2; MDCK-MDR1, Madin−Darby canine kidney cells-multidrug resistance protein 1; MOA, methoxyamine; MW, molecular weight; *P*, plasma concentration; Pgp, P-glycoprotein; PK/PD, pharmacokinetics/pharmacodynamics; pLRRK2, phospho-LRRK2; po, oral administration; P_u, unbound plasma concentration; R, rat; TDI, time-dependent inhibition; TPSA, topological polar surface area; TFA, trifluoroacetic acid; V_d, volume of distribution; XPhos, 2-dicyclohexylphosphino-2′,4′,6′-triisopropylbiphenyl

■ REFERENCES

(1) Lees, A. J.; Hardy, J.; Revesz, T. Parkinson's disease. *Lancet* **2009**, *373*, 2055−2066. Erratum in *Lancet* **2009**, *374*, 684.

(2) Zimprich, A.; Biskup, S.; Leitner, P.; Lichtner, P.; Farrer, M.; Lincoln, S.; Kachergus, J.; Hulihan, M.; Uitti, R. J.; Calne, D. B.; Stoessl, A. J.; Pfeiffer, R. F.; Patenge, N.; Carbajal, I. C.; Vieregge, P.; Asmus, F.; Muller-Myhsok, B.; Dickson, D. W.; Meitinger, T.; Strom, T. M.; Wszolek, Z. K.; Gasser, T. Mutations in LRRK2 cause autosomal-dominant parkinsonism with pleomorphic pathology. *Neuron* **2004**, *44*, 601−607.

(3) Paisan-Ruiz, C.; Jain, S.; Evans, E. W.; Gilks, W. P.; Simon, J.; van der Brug, M.; Lopez de Munain, A.; Aparicio, S.; Gil, A. M.; Khan, N.; Johnson, J.; Martinez, J. R.; Nicholl, D.; Carrera, I. M.; Pena, A. S.; de Silva, R.; Lees, A.; Marti-Masso, J. F.; Perez-Tur, J.; Wood, N. W.; Singleton, A. B. Cloning of the gene containing mutations that cause PARK8-linked Parkinson's disease. *Neuron* **2004**, *44*, 595−600.

(4) Mata, I. F.; Wedemeyer, W. J.; Farrer, M. J.; Taylor, J. P.; Gallo, K. A. LRRK2 in Parkinson's disease: Protein domains and functional insights. *Trends Neurosci.* **2006**, *29*, 286−293.

(5) Greggio, E.; Cookson, M. R. Leucine-rich repeat kinase 2 mutations and Parkinson's disease: Three questions. *ASN Neuro* **2009**, *1*, e00002.

(6) Gandhi, P. N.; Chen, S. G.; Wilson-Delfosse, A. L. Leucine-rich repeat kinase 2 (LRRK2): A key player in the pathogenesis of Parkinson's disease. *J. Neurosci. Res.* **2009**, *87*, 1283−1295.

(7) Dachsel, J. C.; Farrer, M. J. LRRK2 and Parkinson disease. *Arch. Neurol.* **2010**, *67*, 542−547.

(8) Satake, W.; Nakabayashi, Y.; Mizuta, I.; Hirota, Y.; Ito, C.; Kubo, M.; Kawaguchi, T.; Tsunoda, T.; Watanabe, M.; Takeda, A.; Tomiyama, H.; Nakashima, K.; Hasegawa, K.; Obata, F.; Yoshikawa, T.; Kawakami, H.; Sakoda, S.; Yamamoto, M.; Hattori, N.; Murata, M.; Nakamura, Y.; Toda, T. Genome-wide association study identifies common variants at four loci as genetic risk factors for Parkinson's disease. *Nat. Genet.* **2009**, *41*, 1303−1307.

(9) Simón-Sánchez, J.; Schulte, C.; Bras, J. M.; Sharma, M.; Gibbs, J. R.; Berg, D.; Paisan-Ruiz, C.; Lichtner, P.; Scholz, S. W.; Hernandez, D. G.; Krüger, R.; Federoff, M.; Klein, C.; Goate, A.; Perlmutter, J.; Bonin, M.; Nalls, M. A.; Illig, T.; Gieger, C.; Houlden, H.; Steffens, M.;

Okun, M. S.; Racette, B. A.; Cookson, M. R.; Foote, K. D.; Fernandez, H. H.; Traynor, B. J.; Schreiber, S.; Arepalli, S.; Zonozi, R.; Gwinn, K.; van der Brug, M.; Lopez, G.; Chanock, S. J.; Schatzkin, A.; Park, Y.; Hollenbeck, A.; Gao, J.; Huang, X.; Wood, N. W.; Lorenz, D.; Deuschl, G.; Chen, H.; Riess, O.; Hardy, J. A.; Singleton, A. B.; Gasser, T. Genome-wide association study reveals genetic risk underlying Parkinson's disease. *Nat. Genet.* **2009**, *41*, 1308−1312.

(10) West, A. B.; Moore, D. J.; Biskup, S.; Bugayenko, A.; Smith, W. W.; Ross, C. A.; Dawson, V. L.; Dawson, T. M. Parkinson's disease-associated mutations in leucine-rich repeat kinase 2 augment kinase activity. *Proc. Natl. Acad. Sci. U.S.A.* **2005**, *102*, 16842−16847.

(11) Greggio, E.; Jain, S.; Kingsbury, A.; Bandopadhyay, R.; Lewis, P.; Kaganovich, A.; van der Brug, M. P.; Beilina, A.; Blackinton, J.; Thomas, K. J.; Ahmad, R.; Miller, D. W.; Kesavapany, S.; Singleton, A.; Lees, A.; Harvey, R. J.; Harvey, K.; Cookson, M. R. Kinase activity is required for the toxic effects of mutant LRRK2/dardarin. *Neurobiol. Dis.* **2006**, *23*, 329−341.

(12) Cookson, M. R. The role of leucine-rich repeat kinase 2 (LRRK2) in Parkinson's disease. *Nat. Rev. Neurosci.* **2010**, *11*, 791−797.

(13) Rudenko, I. N.; Chia, R.; Cookson, M. R. Is inhibition of kinase activity the only therapeutic strategy for LRRK2-associated Parkinson's disease? *BMC Med.* **2012**, *10*, 20−27.

(14) Liu, Z.; Hamamichi, S.; Lee, B. D.; Yang, D.; Ray, A.; Caldwell, G. A.; Caldwell, K. A.; Dawson, T. M.; Smith, W. W.; Dawson, V. L. Inhibitors of LRRK2 kinase attenuate neurodegeneration and Parkinson-like phenotypes in Caenorhabditis elegans and Drosophila Parkinson's disease models. *Hum. Mol. Genet.* **2011**, *20*, 3933−3942.

(15) Lee, B. D.; Shin, J.-H.; VanKampen, J.; Petrucelli, L.; West, A. B.; Ko, H. S.; Lee, Y.-I.; Maguire-Zeiss, K. A.; Bowers, W. J.; Federoff, H. J.; Dawson, V. L.; Dawson, T. M. Inhibitors of leucine-rich repeat kinase-2 protect against models of Parkinson's disease. *Nat. Med.* **2010**, *16*, 998−1000.

(16) For a recent review on LRRK2 small molecule kinase inhibitors, see Kramer, T.; Lo Monte, F.; Göring, S.; Amombo, G. M. O.; Schmidt, B. Small molecule kinase inhibitors for LRRK2 and their application to Parkinson's disease models. *ACS Chem. Neurosci.* **2012**, *3*, 151−160.

(17) Lee, B. D.; Dawson, V. L.; Dawson, T. M. Leucine-rich repeat kinase 2 (LRRK2) as a potential therapeutic target in Parkinson's disease. *Trends Pharmacol. Sci.* **2012**, *33*, 365−373.

(18) Deng, X.; Dzamko, N.; Prescott, A.; Davies, P.; Liu, Q.; Yang, Q.; Lee, J.-D.; Patricelli, M. P.; Nomanbhoy, T. K.; Alessi, D. R.; Gray, N. S. Characterization of a selective inhibitor of the Parkinson's disease kinase LRRK2. *Nat. Chem. Biol.* **2011**, *7*, 203−205.

(19) Ramsden, N.; Perrin, J.; Ren, Z.; Lee, B. D.; Zinn, N.; Dawson, V. L.; Tam, D.; Bova, M.; Lang, M.; Drewes, G.; Bantscheff, M.; Bard, F.; Dawson, T. M.; Hopf, C. Chemoproteomics-based design of potent LRRK2-selective lead compounds that attenuate Parkinson's disease-related toxicity in human neurons. *ACS Chem. Biol.* **2011**, *6*, 1021−1028.

(20) Nichols, P. L.; Eatherton, A. J.; Bamborough, P.; Jandu, K. S.; Philps, O. J.; Andreotti, D. WO 2011/038572 A1, 2011.

(21) Choi, H. G.; Zhang, J.; Deng, X.; Hatcher, J. M.; Patricelli, M. P.; Zhao, Z.; Alessi, D. R.; Gray, N. S. Brain penetrant LRRK2 inhibitor. *ACS Med. Chem. Lett.* **2012**, *3*, 658−662.

(22) Estrada, A. A.; Liu, X.; Baker-Glenn, C.; Beresford, A.; Burdick, D. J.; Chambers, M.; Chan, B .K.; Chen, H.; Ding, X.; DiPasquale, A. G.; Dominguez, S.; Dotson, J.; Drummond, J.; Flagella, M.; Flynn, S.; Fuji, R.; Gill, A.; Gunzner-Toste, J.; Harris, S.; Heffron, T. P.; Kleinheinz, T.; Lee, D. W.; Le Pichon, C. E.; Lyssikatos, J. P.; Medhurst, A.; Moffat, J. G.; Mukund, S.; Nash, K.; Scearce-Levie, K.; Sheng, Z.; Shore, D. G.; Tran, T.; Trivedi, N.; Wang, S.; Zhang, S.; Zhang, X.; Zhao, G.; Zhu, H.; Sweeney, Z. K. Discovery of highly potent, selective and brain-penetrable Leucine-Rich Repeat Kinase 2 (LRRK2) small molecular inhibitors. *J. Med. Chem.* **2012**, *55*, 9416−9433.

(23) Chen, H.; Chan, B. K.; Drummond, J.; Estrada, A. A.; Gunzner-Toste, J.; Liu, X.; Liu, Y.; Moffat, J. G.; Shore, D.; Sweeney, Z. K.; Tran, T.; Wang, S.; Zhao, G.; Zhu, H.; Burdick, D. J. Discovery of selective LRRK2 inhibitors guided by computational analysis and molecular modeling. *J. Med. Chem.* **2012**, *55*, 5536−5545.

(24) Zabierek, A. A.; Konrad, K. M.; Haidle, A. M. A practical, two-step synthesis of 1-alkyl-4-aminopyrazoles. *Tetrahedron Lett.* **2008**, *49*, 2996−2998.

(25) Ritchie, T. J.; Macdonald, S. J. F.; Peace, S.; Pickett, S. D.; Luscombe, C. N. The developability of heteroaromatic and heteroaliphatic rings—Do some have a better pedigree as potential drug molecules than others? *Med. Chem. Commun.* **2012**, *3*, 1062−1069.

(26) In general, there was no evidence of inhibition of the other major CYP isoforms by the pyrazole inhibitors.

(27) For details of the pLRRK2 cellular assay: Sheng, Z.; Zhang, S.; Bustos D.; Kleinheinz, T.; Le Pichon, C. E.; Dominguez, S.; Solanoy, H. O.; Drummond, J.; Zhang, X.; Ding, X.; Li, X.; Yue, Z.; Liu, X.; Burdick, D. J.; Estrada, A. A.; Gunzner-Toste, J.; Chen, H.; Sweeney, Z. K.; Scearce-Levie, K.; Moffat, J. G.; Kirkpatrick, D. S.; Zhu, H. Autophosphorylation of Ser 1292 on LRRK2 is an in vivo biomarker of kinase activity and is required for LRRK2-induced neuronal toxicity. *Sci. Transl. Med.*, in press.

(28) Waring, M. J. Lipophilicity in drug discovery. *Expert Opin. Drug Discovery* **2010**, *5*, 235−248.

(29) For a review on CYP1A2, see Shu-Feng, Z.; Wang, B.; Yang, L.-P.; Liu, J.-P. Structure, function, regulation and polymorphism and the clinical significance of human cytochrome P450 1A2. *Drug Metab. Rev.* **2010**, *42*, 268−354.

(30) Sansen, S.; Yano, J. K.; Reynald, R. L.; Schoch, G. A.; Griffin, K. J.; Stout, C. D.; Johnson, E. F. Adaptations for the oxidation of polycyclic aromatic hydrocarbons exhibited by the structure of human P450 1A2. *J. Biol. Chem.* **2007**, *282*, 14348−14355.

(31) Li, X.; Patel, J. C.; Wang, J.; Avshalumov, M. V.; Nicholson, C.; Buxbaum, J. D.; Elder, G. A.; Rice, M. E.; Yue, Z. Enhanced striatal dopamine transmission and motor performance with LRRK2 overexpression in mice is eliminated by familial Parkinson's disease mutation G2019S. *J. Neurosci.* **2010**, *30*, 1788−1797.

(32) Compound **18** was dosed intraperotineal (ip) at 10 or 15 mg/kg (n = 3/dose) as a 1% Avicel RC-591 suspension. Tissues were harvested at 1, 3, and 6 h postdose to assess pSer1292 levels and compound concentration as previously described in ref 27. The in vivo pLRRK2 inhibition vs unbound plasma and brain concentration data were fitted with the following equation using WinNonlin (Pharsight): $E = (E_{max} - E_p) \times IC_{50}/(IC_{50} + C)$, where E represents the remaining brain pLRRK2 activity as compared to the vehicle-treated group following the treatment, E_{max} represents maximal activity of pLRRK2, E_p represents residual activity, IC_{50} represents unbound plasma or brain concentrations that inhibit 50% of pLRRK2 in the brain, and C represents unbound brain concentration.

(33) Chang, S.; Zhang, L.; Xu, S.; Luo, J.; Lu, X.; Zhang, Z.; Xu, T.; Liu, Y.; Tu, Z.; Ren, X.; Geng, M.; Ding, J.; Pei, D.; Ding, K. Design, synthesis, and biological evaluation of novel conformationally constrained inhibitors targeting epidermal growth factor receptor threonine^{790}→methionine^{790} Mutant. *J. Med. Chem.* **2012**, *55*, 2711−2723.

(34) Breslin, H. J.; Lane, B. M.; Ott, G. R.; Ghose, A. K.; Angeles, T. S.; Albom, M. S.; Cheng, M.; Wan, W.; Haltiwanger, R. C.; Wellas-Knecht, K. J.; Dorsey, B. D. Design, synthesis, and anaplastic lymphoma kinase (ALK) inhibitory activity for a novel series of 2,4,8,22-tetraazatetracyclo[14.3.1.1^{3,7}.1^{9,13}]-docosa-1(20), 3(22),4,6,9(21),10,12,16,18-nonaene macrocycles. *J. Med. Chem.* **2012**, *55*, 449−464.

(35) Gingrich, D. E.; Lisko, J. G.; Curry, M. A.; Cheng, M.; Quail, M.; Lu, L.; Wan, W.; Albom, M. S.; Angeles, T. S.; Aimone, L. D.; Haltiwanger, R. C.; Wells-Knecht, K.; Ott, G. R.; Ghose, A. K.; Ator, M. A.; Ruggeri, B.; Dorsey, B. D. Discovery of an orally efficacious inhibitor of anaplastic lymphoma kinase. *J. Med. Chem.* **2012**, *55*, 4580−4593.

(36) Chen, S.; Bartkovitz, D.; Cai, J.; Chen, Y.; Chen, Z.; Chu, X.-J.; Le, K.; Le, N. T.; Luk, K.-C.; Mischke, S.; Naderi-Oboodi, G.; Boylan,

J. F.; Nevins, T.; Qing, W.; Chen, Y.; Wovkulich, P. M. Identification of novel, potent and selective inhibitors of Polo-like kinase 1. *Bioorg. Med. Chem. Lett.* **2012**, *22*, 1247−1250.